Single-Molecule-Magnet Carbon-Nanotube Hybrids**

Lapo Bogani,* Chiara Danieli, Elisa Biavardi, Nedjma Bendiab, Anne-Laure Barra, Enrico Dalcanale, Wolfgang Wernsdorfer, and Andrea Cornia

Dedicated to an anonymous bone-marrow donor in Cyprus

Carbon nanotubes (CNTs) hold great promise for sensing[1,2] and nanoelectronics,[3] as core components of chemical and biological[1,2] ultra-sensitive probes and of field-effect transistors (FETs).[3] CNT–SQUID devices[4] in particular could constitute magnetic detectors with single-molecule sensitivity, thus offering a viable route to the long-sought readout of magnetic information stored in individual single-molecule magnets (SMMs).[5] SMMs are metal-ion clusters with a large easy-axis magnetic anisotropy,[6] exhibiting a magnetic hysteresis loop at low temperature and suggested as components for quantum computing[7] and molecular spintronics.[5] To date, the chemistry needed to bridge the domains of CNTs and SMMs has remained unexplored. CNT hybrids with gold or magnetic nanoparticles, proteins, enzymes, or luminescent molecules are currently under intense investigation.[1,2,8] The resulting materials usually entail a large number of nanoparticles or molecules per CNT, whereas CNT–SMM detectors and spintronic devices require the sequential addition of a small but very controlled number of nanomagnets. Grafting through covalent bonds might introduce electron scattering centers that may limit the performance of CNT devices. By contrast, noncovalent π-stacking interactions with pristine CNTs should largely preserve the CNT conductance, while guaranteeing SMM–CNT interaction.

Herein we report the assembly of CNT–SMM hybrids using a tailor-made tetrairon(III) SMM, [Fe$_4$(L)$_2$(dpm)$_6$] (**1**; Hdpm = dipivaloylmethane), designed to graft onto the walls of CNTs. The ligand L^{3-} (H$_3$L = 2-hydroxymethyl-2-(4-(pyren-1-yl)butoxy)methylpropane-1,3-diol), features an alkyl chain with a terminal pyrenyl group and was synthesized as in Figure 1a. Reduction of 4-pyren-1-yl-butyric acid gives 4-(1-pyrenil)butanol, which is then coupled with 4-bromomethyl-1-methyl-2,6,7-trioxa-bicyclo[2.2.2]octane.[9] A two-steps deprotection of the trimethylol function affords H$_3$L, which is finally treated with the preformed[6] complex [Fe$_4$-(OMe)$_6$(dpm)$_6$] (**2**) to give **1** in excellent yield (95%).

The molecular structure of **1** (Figure 1 b,c), determined by single-crystal X-ray diffraction,[10] shows a tetrairon(III) propeller-like core with idealized D_3 symmetry held together by two triply deprotonated H$_3$L ligands lying at opposite sides of the molecular plane (see Supporting Information). The molecular size of **1** is 1.6–2.3 nm (av.: 1.9 nm). Low-temperature high-frequency (HF)-EPR spectra at 190 and 230 GHz (Figure 2a) and variable-temperature magnetic-susceptibility measurements show the presence of an $S = 5$ high-spin ground state with an easy-axis magnetic anisotropy ($D = -0.409$ cm^{-1}; Supporting Information). Indeed, single-crystal magnetic measurements reveal a hysteresis loop below 1 K with characteristic quantum-tunneling[6] steps (Figure 2 b), confirming the SMM behavior.

CNT–FETs were obtained by electron-beam lithography on degenerately n-doped silicon wafers covered with a 300 nm thick SiO$_2$ layer. Single CNTs were located by atomic force microscopy (AFM) and connected by palladium leads separated by 300 nm gaps. The hybrids were then produced by immersion of the CNT–FETs in a 3.1×10^{-5} M solution of **1** in 1,2-dichloroethane (DCE) for 30 min, followed by extensive washing with pure DCE. ^{1}H NMR, ESI-MS, and fluorescence techniques demonstrate that the complex is completely stable in solution in the conditions used for the deposition (Supporting Information). The grafting was reiterated to follow the progressive addition of SMMs. After each treatment a few SMMs were found to stick onto the CNT (Figure 3a), while some others were also located on the surrounding surface. The isostructural complex containing H$_3$L' = 2-hydroxymethyl-2-phenylpropane-1,3-diol[11] did not graft onto CNTs in the same experimental conditions. This result is a strong indication that **1** has been grafted as a result of the pyrenyl functionalities.

[*] Dr. L. Bogani, Dr. N. Bendiab, Dr. W. Wernsdorfer
Institut Néel, CNRS
25 Av. des Martyrs, 38042 Grenoble, Cedex 9 (France)
Fax: (+33) 4-7688-1191
E-mail: lbogani@hotmail.com

Dr. A.-L. Barra
LCMI-CNRS
25 Av. des Martyrs, 38042 Grenoble, Cedex 9 (France)

Dr. C. Danieli, Prof. A. Cornia
Dipartimento di Chimica & INSTM
Università di Modena e Reggio Emilia
Via G. Campi 183, 41100 Modena (Italy)

Dr. E. Biavardi, Prof. E. Dalcanale
Dipartimento di Chimica Organica e Industriale & INSTM
Università di Parma
Viale G. P. Usberti 17/a, 43100 Parma (Italy)

Supporting information for this article is available on the WWW under http://dx.doi.org/10.1002/anie.200804967.
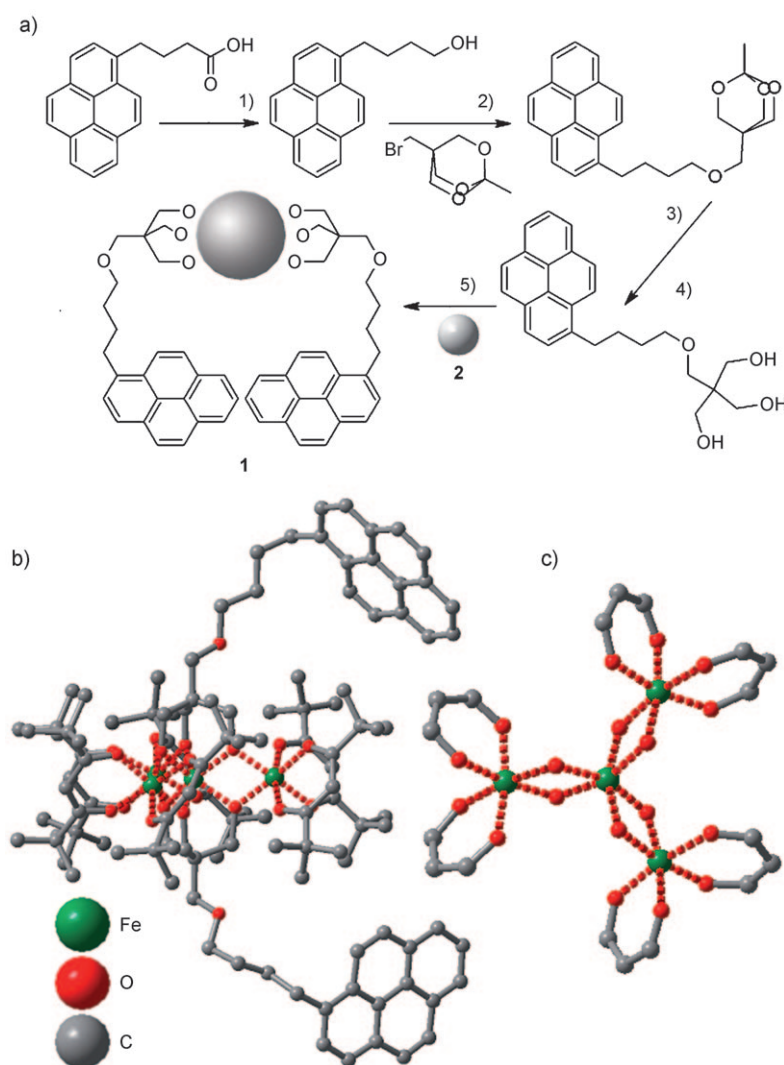
Figure 1. a) Synthesis of **1**: 1) BH$_3$·THF, THF, 0°C, 20 h, 2) NaOH, DMF, 90°C, 12 h, 3) HCl, MeOH, 6 h, 4) Na$_2$CO$_3$, MeOH, 12 h, 5) Et$_2$O, [Fe$_4$(OMe)$_6$(dpm)$_6$] (**2**). b) Crystal structure of **1**, showing the Fe$_4$ core and the peripheral pyrene-terminated chains (hydrogen atoms omitted). c) View of the tetrairon(III) core along the idealized three-fold axis, showing the preserved cluster geometry (ligands H$_3$L and *tert*-butyl carbon atoms of dpm omitted).

Fe
O
C

Micro-Raman investigation of the CNT–SMM hybrids clearly revealed, superimposed onto CNT and SiO$_2$ spectra, several peaks associated with intact molecules of **1**. They are not observed when the solutions used in the deposition are thermally treated so as to intentionally break the SMM magnetic core (Supporting Information). Furthermore, the fluorescence of pyrene units is quenched in the hybrids, as in solutions of intact **1** (Supporting Information).

If **1** is randomly distributed along the CNT the probability of having two consecutive molecules at a distance L is $P(C,L) = C e^{-LC}$, where C is the linear concentration of **1** on CNTs.[12] Statistical analysis of the distribution of L, performed on 40 CNTs, revealed good agreement with the predicted law and allowed C to be extracted for each repetition (Figure 4). C varies linearly ($R = 0.998$) with the number of repetitions, with 1.5 SMM μm^{-1} deposited at each iteration. Thus, in CNT–FETs with 300 nm gaps, we can graft, on average, one SMM every two treatments, allowing the sequential addition of single SMMs to CNT devices.

CNTs are either metallic or semiconducting. Herein we concentrate on the room-temperature transport properties of devices based on semiconducting CNTs, which are better suited for ultra-sensitive detection.[2,3] Current (I_d) versus gate voltage (V_g) curves show p-type FET behavior[4] (ON state at $V_g < 0$) with typical I_{ON}/I_{OFF} ratios of three decades (Figure 5a). Hysteresis is observed, as a result of charge injection from the CNT to the nearby region.[13] The subthreshold swing $S_w = [dV_g/dLog(I)]$ remains unchanged upon grafting, indicating that the treatment leaves the gate unaffected. While no appreciable variation is observed after repeated treatment of the FETs with DCE alone (Supporting Information), the I_{ON} current decreases linearly upon SMM grafting, indicating that **1** interacts with the electron flow, producing scattering centers.[3] Linear fit of the trend ($R = 0.989$) indicates a contribution of 560 ± 40 pA per SMM (Figure 5b), which is higher than our instrumental sensitivity of 10 pA and demonstrates single-molecule detection capability. In the Landauer formulation of incoherent transport regime,[14] such I_{ON} decrease corresponds to an electron reflection coefficient of about 7% per SMM. For comparison, covalent binding of protein molecules on CNTs leads to an electron reflection coefficient of 40% per molecule.[3]

The grafting also produces a gradual decrease in the ON/OFF threshold voltage V_{th1}, along with an increase of the hysteresis width (Supporting Information). This change is to be attributed to charge-trapping by **1**, as well as a charge transfer between **1** and the CNT.

Interestingly **1** can be burnt by laser irradiation (30 mW μm^{-2} at 576.5 nm), causing the disappearance of the

The AFM height profile of the same CNT reveals the sequential addition, after each treatment, of objects with size of 1–2 nm (Figure 3b). Statistical analysis of small CNTs with diameter of about 1 nm (Figure 3c) shows a two-peak distribution that can be fitted ($R^2 = 0.98$) with two Gaussians centered at (1.9 ± 0.3) nm and (1.0 ± 0.3) nm (errors are full-widths-at-half-maxima), with an area ratio of 1:3.

The former peak closely matches the molecular size evaluated from X-ray data and can be assigned to SMMs lying on top of CNTs. The feature of height 1 nm most likely arises from SMMs lying beside a CNT, for which the CNT–SMM height difference is detected (Figure 3d), because of the limited lateral resolution of the AFM tip. Thus about ¼ of the grafted SMMs rest on top of the CNTs, with no direct interaction with the surface. Inspection of CNTs or bundles with diameter larger than 2 nm shows only one Gaussian peak ($R^2 = 0.993$) at 2.0 ± 0.2 nm, confirming this interpretation.
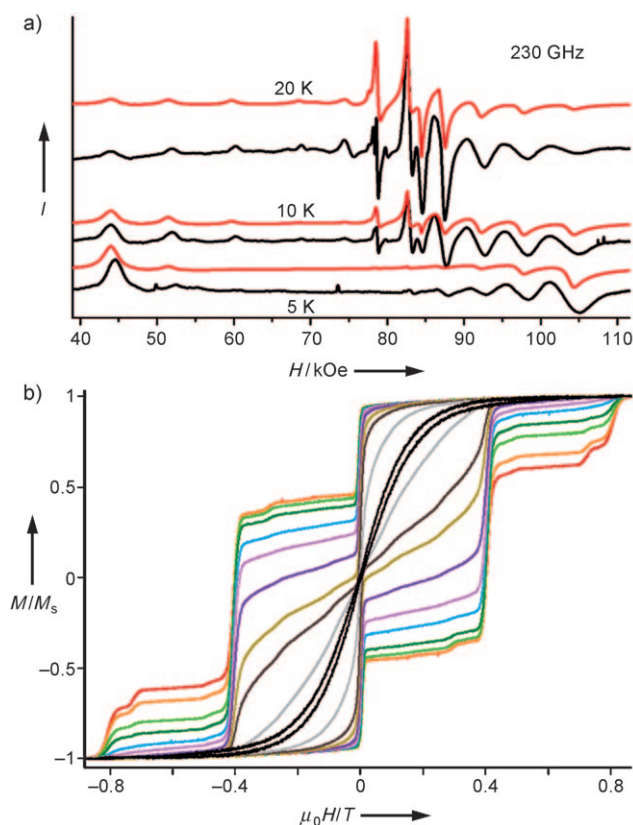
Figure 2. Magnetic properties of **1**: a) Variable-temperature HF-EPR spectra recorded at 230 GHz (black) on a powder sample, along with the best-fit simulations (red); b) Hysteresis cycles recorded on a single crystal of **1** at 11 different temperatures between 1 K (black) and 40 mK (red). The magnetic field is swept at a rate of 170 Oe s^{-1} along the magnetic easy axis.

Figure 3. AFM topographic analysis of the hybrids. a) Height images of the same CNT acquired on repeating the grafting process: left one time, center four times, right ten times. b) Section profile along the same CNT before (black line) and after (red line) multiple grafting of **1**. c) Heights of the grafted objects. The statistics acquired on single CNTs or small bundles with diameter <1 nm (yellow; 1 & 2 see (d)) differs from that acquired on CNTs or bundles with larger diameter (blue; 3 & 4 see (d)). Lines are fittings with Gaussian distributions. d) Corresponding different dispositions of **1** with respect to CNTs (1 & 2) or bundles (3 & 4).

Raman fingerprints and the recovery the original transport curve (Figure 5a). The grafting–burning procedure can be repeated up to a dozen times, but after this point further iterations fail to recover the original curve, probably because of accumulation of depleted material.

In conclusion we bridged the domains of molecular magnetism and CNTs by fabricating the first CNT–SMMs hybrids containing intact pyrene-functionalized SMMs in conditions compatible to the creation of electronic devices. We controlled the grafting of SMMs down to a single-molecule level and we demonstrated the single-SMM sensitivity of CNT–FETs. These results pave the way to the construction of "double-dot" molecular spintronic devices,[5] where a controlled number of nanomagnets is coupled to an electronic nanodevice, and to the observation of the magneto-Coulomb effect. The future use of CNT–SQUIDs may also benefit from the chemical methodology described herein. Finally, the approach may be extended to produce different functional hybrids incorporating charge-transfer complexes, valence tautomers, or photomagnetic materials.[15]
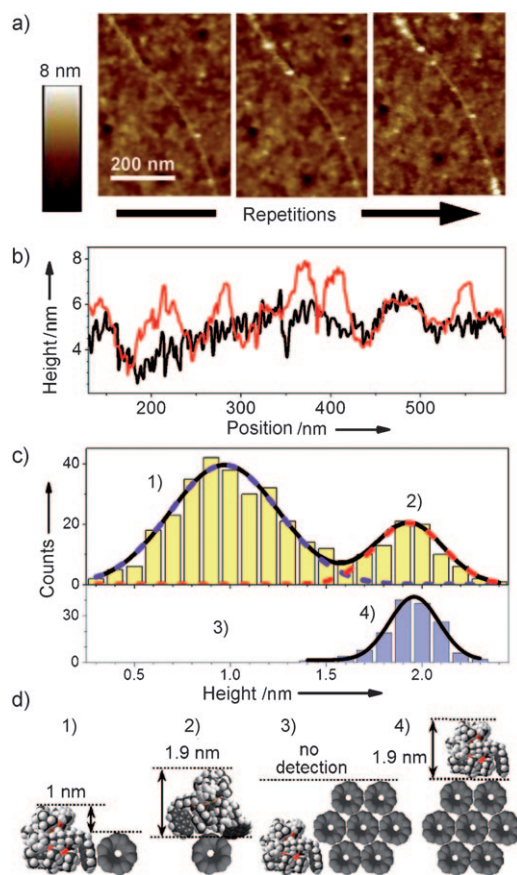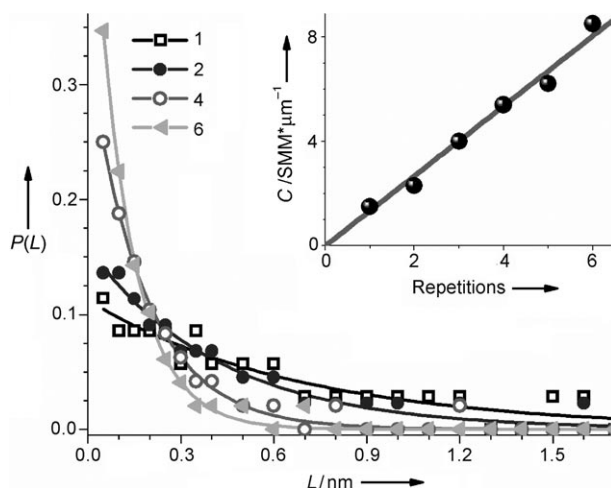

Figure 4. Probability of finding a distance L between SMMs grafted on CNTs for sequential repetitions of the process. Symbols are experimental data for 1, 2, 4, and 6 repetition and lines are the corresponding fits (see text). Inset: extracted linear concentration (C) as a function of the number of repetitions of the process and linear fit.
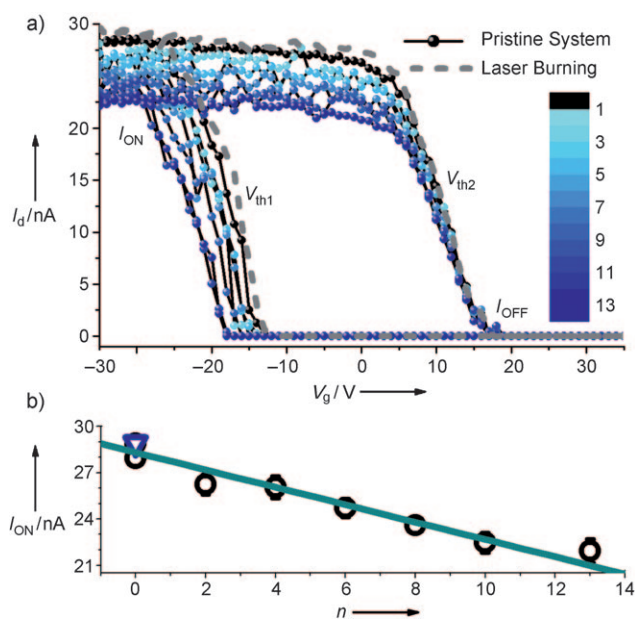
Figure 5. Transport properties of the SMM–CNT hybrids. a) I_d versus V_g curve of a typical CNT–FET shown for the pristine device (black line) and for different numbers (n) of grafted SMMs (color scale). The original curve is regained after destruction of **1** by laser burning (gray dashed line) V_{th1} and V_{th2} indicate the ON→OFF and OFF→ON threshold voltages, respectively. b) Variation of the I_{ON} as a function of the number of grafted molecules (n; circles). The triangle represents the value after laser burning and the line is a fit to the data.

Experimental Section

Detailed description of the synthetic procedures is reported in the Supporting Information. CNT–FETs were fabricated on degenerately n-doped Si wafers covered with 300 nm thick SiO_2 (Siltronix sas). Gold electrodes were deposited on the surface by deep-UV lithography, providing a reference system to locate CNTs. Single-walled CNTs (Rice Univ.) in DCE were spin-coated on the wafers, located by AFM and connected with Pd leads by e-beam lithography (Supporting Information). 65% of contacts displayed a resistance lower than 100 kΩ. AFM images were acquired using a Veeco D3100 instrument in tapping mode; hysteresis loops and HF-EPR spectra were recorded on home-built instrumentation;[11] Raman spectra at 632.8 nm were obtained on a LabRam Infinity spectrometer focusing on an area of $1 \mu m^2$.

[1] a) J. Kong, N. R. Franklin, C. Zhou, M. G. Chapline, S. Peng, K. Cho, H. Dai, *Science* **2000**, *287*, 622–625; b) P. G. Collins, K. Bradley, M. Ishigami, A. Zettl, *Science* **2000**, *287*, 1801–1804; c) K. Besteman, J.-O. Lee, F. G. M. Wiertz, H. A. Heering, C. Dekker, *Nano Lett.* **2003**, *3*, 727–730; d) A. Star, J. C. P. Gabriel, K. Bradley, G. Gruner, *Nano Lett.* **2003**, *3*, 459–462; e) R. J. Chen, S. Bangsaruntip, K. A. Drouvalakis, N. Wong Shi Kam, M. Shim, Y. Li, W. Kim, P. J. Utz, H. Dai, *Proc. Natl. Acad. Sci. USA* **2003**, *100*, 4984–4989.

[2] Y. B. Zhang, M. Kanungo, A. J. Ho, P. Freimuth, D. van der Le-lie, M. Chen, S. M. Khamis, S. S. Datta, A. T. C. Johnson, J. A. Misewich, S. S. Wong, *Nano Lett.* **2007**, *7*, 3086–3091.

[3] a) M. Ouyang, J.-L. Huang, C. L. Cheung, C. M. Lieber, *Science* **2001**, *292*, 702–705; b) P. Avouris, Z. Chen, V. Perebeinos, *Nat. Nanotechnol.* **2007**, *2*, 605–615; c) S. J. Tans, A. R. M. Verscheu-ren, C. Dekker, *Nature* **1998**, *393*, 49–52; d) D. N. Futaba, K. Hata, T. Yamada, T. Hiraoka, Y. Hayamizu, Y. Kakudate, O. Tanaike, H. Hatori, M. Yumura, S. Iijima, *Nat. Mater.* **2006**, *5*, 987–994.

[4] SQUID = superconducting quantum interference device; a) J.-P. Cleuziou, W. Wernsdorfer, V. Bouchiat, T. Ondarçuhu, M. Monthioux, *Nat. Nanotechnol.* **2006**, *1*, 53–59; b) P. Jarillo-Herrero, J. A. van Dam, L. P. Kouwenhoven, *Nature* **2006**, *439*, 953–956.

[5] a) L. Bogani, W. Wernsdorfer, *Nat. Mater.* **2008**, *7*, 179–186; b) L. Bogani, W. Wernsdorfer, *Inorg. Chim. Acta* **2008**, *361*, 3807–3819.

[6] a) D. Gatteschi, R. Sessoli, J. Villain, *Molecular Nanomagnets*, Oxford University Press, Oxford, UK, **2006**; b) D. Gatteschi, R. Sessoli, *Angew. Chem.* **2003**, *115*, 278–309; *Angew. Chem. Int. Ed.* **2003**, *42*, 268–297; c) A. L. Barra, A. Caneschi, A. Cornia, F. F. De Biani, D. Gatteschi, C. Sangregorio, R. Sessoli, L. Sorace, *J. Am. Chem. Soc.* **1999**, *121*, 5302–5310.

[7] a) M. N. Leuenberger, D. Loss, *Nature* **2001**, *410*, 789; b) F. Troiani, A. Ghirri, M. Affronte, S. Carretta, P. Santini, G. Amoretti, S. Piligkos, G. Timco, R. E. P. Winpenny, *Phys. Rev. Lett.* **2005**, *94*, 207208; c) F. Troiani, M. Affronte, S. Carretta, P. Santini, G. Amoretti, *Phys. Rev. Lett.* **2005**, *94*, 190501; d) J. Lehmann, A. Gaita-Ariño, E. Coronado, D. Loss, *Nat. Nano-technol.* **2007**, *2*, 312–317.

[8] a) S. Banerjee, T. Hemraj-Benny, S. S. Wong, *Adv. Mater.* **2005**, *17*, 17–29; b) D. M. Guldi, G. M. A. Rahman, F. Zerbetto, M. Prato, *Acc. Chem. Res.* **2005**, *38*, 871–878; c) V. Georgakilas, D. Gournis, V. Tzitzios, L. Pasquato, D. Guldi, M. Prato, *J. Mater. Chem.* **2007**, *17*, 2679–2694; d) K. Kurppa, H. Jiang, G. R. Szilvay, A. G. Nasibulin, E. I. Kauppinen, M. B. Linder, *Angew. Chem.* **2007**, *119*, 6566–6569; *Angew. Chem. Int. Ed.* **2007**, *46*, 6446–6449; e) K. Jiang, A. Eitan, L. S. Schadler, P. M. Ajayan, R. W. Siegel, N. Grobert, M. Mayne, M. Reyes-Reyes, H. Terrones, M. Terrones, *Nano Lett.* **2003**, *3*, 275–277.

[9] A. B. Padias, H. K. Hall, *Macromolecules* **1982**, *15*, 217–223.

[10] Crystal structure data for **1**: $C_{116}H_{164}Fe_4O_{20}$, $M_r = 2101.87$, crystal dimensions $0.64 \times 0.42 \times 0.30$ mm, triclinic, space group $P\bar{1}$, $a = 16.3398(4)$, $b = 19.1784(5)$, $c = 21.9168(5)$ Å, $\alpha = 87.025(1)°$, $\beta = 68.784(1)°$, $\gamma = 65.182(1)°$, $V = 5770.6(2)$ Å^3, $Z = 2$, $\rho_{calcd} = 1.210$ g cm^{-3}, $\mu = 0.556$ mm^{-1}, Mo$_{K\alpha}$ radiation, $\lambda = 0.71073$ Å, $T = 120(2)$ K, $2\theta_{max} = 50.16°$, 42131/19160 reflections collected/ unique ($R_{int} = 0.0264$), $R1 = 0.0733$, $wR2 = 0.2323$, largest diff. peak and hole $0.985/-0.558$ e Å^{-3}. CCDC-704776 (**1**) contains the supplementary crystallographic data for this paper. These data can be obtained free of charge from The Cambridge Crystallographic Data Centre via www.ccdc.cam.ac.uk/data_request/cif.

[11] S. Accorsi, A.-L. Barra, A. Caneschi, G. Chastanet, A. Cornia, A. C. Fabretti, D. Gatteschi, C. Mortalò, E. Olivieri, F. Parenti, P. Rosa, R. Sessoli, L. Sorace, W. Wernsdorfer, L. Zobbi, *J. Am. Chem. Soc.* **2006**, *128*, 4742–4755.

[12] a) N. L. Johnson, S. Kotz, *Distributions in Statistics*, Wiley, New York, **1972**; b) For the conceptually identical problem of randomly placed diamagnetic sites in a magnetic chain, see: L. Bogani, A. Caneschi, M. Fedi, D. Gatteschi, M. Massi, M. A. Novak, M. G. Pini, A. Rettori, R. Sessoli, A. Vindigni, *Phys. Rev. Lett.* **2004**, *92*, 207204; c) L. Bogani, R. Sessoli, M. G. Pini, A. Rettori, M. A. Novak, M. Massi, M. Fedi, L. Giuntini, A. Caneschi, D. Gatteschi, *Phys. Rev. B* **2005**, *72*, 064405.

[13] a) K. Bradley, J. Cumings, A. Star, J.-C. P. Gabriel, G. Gruner, *Nano Lett.* **2003**, *3*, 639–641; b) W. Kim, A. Javey, O. Vermesh, Q. Wang, Y. Li, H. Dai, *Nano Lett.* **2003**, *3*, 193–198.

[14] a) M. Bockrath, W. Liang, D. Bozovic, J. H. Hafner, C. M. Lieber, M. Tinkham, H. Park, *Science* **2001**, *291*, 283–285; b) A. Bachtold, M. S. Fuhrer, S. Plyasunov, M. Forero, E. H. Anderson, E. Zettl, P. L. McEuen, *Phys. Rev. Lett.* **2000**, *84*, 6082–6085.

[15] a) J. S. Miller, J. C. Calabrese, R. S. McLean, A. J. Epstein, *Adv. Mater.* **1992**, *4*, 490–493; b) A. Dei, *Angew. Chem.* **2005**, *117*, 1184–1187; *Angew. Chem. Int. Ed.* **2005**, *44*, 1160–1163; c) C. Carbonera, A. Dei, J.-F. Létard, C. Sangregorio, L. Sorace, *Angew. Chem.* **2004**, *116*, 3198–3200; *Angew. Chem. Int. Ed.* **2004**, *43*, 3136–3138; d) K. Matsuda, M. Irie, *J. Am. Chem. Soc.* **2000**, *122*, 8309–8310.